

A perturbational study of some hydrogen-bonded dimers

Jacqueline Langlet,^{a)} Jacqueline Caillet,^{b)} and Michel Caffarel^{c)}
CNRS-Laboratoire de Dynamique des Interactions Moléculaires, Université Paris VI,
Tour 22 4 Place Jussieu 75252 Paris Cedex 05, France

(Received 31 January 1995; accepted 31 July 1995)

We present a detailed study of several hydrogen-bonded dimers consisting of H₂O, NH₃, and HF molecules using the Symmetry Adapted Perturbation Theory (SAPT) at different levels of approximations. The relative importance of each individual perturbational components and the quality of the total interaction energies obtained are discussed. The dependence of the results on the relative orientation of the molecules of the dimers and on the intermonomer distance is also investigated. © 1995 American Institute of Physics.

I. INTRODUCTION

It is well-known that evaluating intermolecular interaction energies with the level of accuracy required by the physics and chemistry of complex molecular systems is very difficult. There are two basic reasons for that. First, the interaction energy (defined as the difference between the total energy of the complex and the sum of the total energies of the individual noninteracting species) is really a tiny fraction of the total energies involved. Typically, this fraction can vary from about 10⁻⁷ (weakly interacting van der Waals complexes) to about 10⁻⁴ (strong hydrogen-bonded systems). Second, there is no *exact* method to compute *directly* this very small difference. In absence of such a procedure, two different theoretical strategies are usually employed. A first natural strategy consists in computing the total energy of each species separately (the complex and the individual molecules) and then to subtract out these energies according to the very definition of the interaction energy (the so-called *supermolecular* method). To do that is difficult due to the very high level of control required on the different sources of approximation of the particular method used to compute the total energies. Without entering into the technical details (choice of the basis set functions, finite-basis-set error, basis set superposition error (BSSE), etc...) it is fair to say that current state-of-the-art *ab initio* calculations are not able to reach the necessary level of accuracy, except of course for very small interacting species. A second quite natural approach is to consider that the interaction energy is the result of a very small physical perturbation of the isolated monomers and thus to employ some kind of perturbational method. This line of research has been intensively followed during the last decades and has led to the so-called Symmetry Adapted Perturbation Theories (SAPT) (see e.g., Refs. 1, 2, or 3), a variety of methods based on the usual Rayleigh–Schrödinger perturbation theory supplemented by some technique to force the change of antisymmetry property of the wave function between the monomers and the interacting complex (as known there is not a unique way to do that and, then, various schemes have been proposed, see references in Ref. 1). It is this constraint which is at the origin of the strong repulsion at short distances (exchange contributions).

In order to take account of the continuum contribution present in the infinite sums involved in the perturbational components (except, of course, for the first-order), a variation-perturbation scheme is usually employed (it can be shown that this can be reduced to a calculation in a suitable dimer basis set).^{4,5} In their pioneering work on the use of SAPT Jeziorski and van Hemert (JvH)⁴ have proposed to compute the interaction energy using the following minimal representation:

$$\Delta E_{int} \sim E_{RS}^{(1)} + E_{exch}^{(1)} + E_{ind}^{(2)} + E_{disp}^{(2)}, \quad (1)$$

where all quantities are computed using the wave functions issued from a SCF calculation of the monomers. $E_{RS}^{(1)}$ is the standard Rayleigh–Schrödinger first-order component (physically, the classical electrostatic interaction of the unperturbed charge distributions in the monomers), $E_{exch}^{(1)}$ is the first-order exchange part resulting from the change of the antisymmetry property of the wave function (physically, the dominant part of the repulsive interaction at short distances) and where $E_{ind}^{(2)}$ and $E_{disp}^{(2)}$ are the second-order Rayleigh–Schrödinger induction and dispersion energy, respectively (physically, the energy of interaction of one monomer within the electric field of the other, and the major attractive contribution to the interaction energy for neutral systems, respectively). It is important to emphasize that Eq. (1) describes the main physical facts of the intermolecular interaction (electrostatic interaction, repulsive force, induction and dispersive forces). However, a number of corrections are neglected when using Eq. (1). The numerical experience shows that their importance is very system-dependent. It is therefore very important to compute them if a reliable (although approximate) answer for any interacting system and not just for a specific class of systems is wanted. Three types of corrections may be distinguished:

- (i) corrections to the exchange part due to effects beyond the first-order,
- (ii) corrections due to higher-order perturbational Rayleigh–Schrödinger components ($E_{RS}^{(n)}$ with $n > 2$),
- (iii) corrections due to the intramolecular correlation effects.

A great deal of activity has been devoted to the calculation of these corrections. First of all, it has been very soon realized that the first-order exchange contribution was not sufficient to give a proper description of the repulsive part at

^{a)}E-mail: jl@dim.jussieu.fr

^{b)}E-mail: jc@dim.jussieu.fr

^{c)}E-mail: mc@dim.jussieu.fr

intermediate distances and different methods have been proposed to evaluate the second-order exchange contributions.^{5–12} Note that at much shorter distances no satisfactory approach seems to exist.¹³ Incorporating these important contributions we arrive at the following decomposition

$$\Delta E_{int}^{SAPT} \sim E_{RS}^{(1)} + E_{exch}^{(1)} + E_{ind}^{(2)} + E_{exch-ind}^{(2)} + E_{disp}^{(2)} + E_{exch-disp}^{(2)}, \quad (2)$$

which we shall refer to in the following as the SAPT decomposition. An alternative way of going beyond Eq. (1) is to combine both perturbational and supermolecular worlds as follows:

$$\Delta E_{int}^{hybrid} \sim \Delta E_{SCF} + E_{disp}^{(2)} + E_{exch-disp}^{(2)}, \quad (3)$$

where ΔE_{SCF} is the SCF binding energy computed with the supermolecular method (corrected for the BSSE). Such a procedure is attractive since the SCF interaction energy is supposed to contain most of the second-order exchange-induction energy, some induction part of third- and higher-order perturbational terms and even some intramolecular correlation contribution introduced when doing a SCF supermolecular calculation,¹⁴ contributions which are all neglected when using Eq. (1). In the following we shall refer to it as the *hybrid* method. However, when resorting to Eq. (3) it is important to realize that mixing both approaches renders difficult the control on the errors made. How much of the higher-order perturbational contributions, what part of the exchange-induction energy, etc... is gotten with a SCF supermolecular calculation is not easy to estimate. Note that it can be argued that a pure perturbational treatment where individual errors are in a better control may be preferable. In the same idea of incorporating nonperturbational effects it has been proposed to include the so-called apparent correlation or self-consistency effects into the second-order induction energy, $E_{ind}^{(2)}$.^{15–18} In short, it consists in resorting to a coupled Hartree-Fock (CHF) which implicitly sums up to infinity certain diagrams appearing in the many-body expansion of the induction energy. This is expected to give a better approximation of the total induction energy. Note that this can also be done for the exchange-induction part.¹⁹ Concerning the explicit calculation of higher-order perturbational components very little is found in the literature (see, references in Refs. 1,20,21). Finally, let us note that very recently a great deal of attention has been focused on the calculation of intramolecular correlation contributions to the interaction energy.^{11,13,20,22–28} The monomer Hamiltonians are decomposed as a sum of the Fock operator and some residual intramonomer correlation operator (Møller-Plesset partitioning). Using a many-body expansion framework a double perturbation theory (in the correlation operators of each monomer) may be written down for any of the interaction components. Some calculations of the leading corrections to the first- and second-order perturbational components have been presented (see previous references). Note also that quantum Monte Carlo (QMC) techniques can be used to compute *exactly* perturbational quantities (in particular, the intramonomer correlation effects can be fully taken into ac-

count, see application to the He–He interaction in Refs. 21,29). However, it should be noted that the method is in practice limited to the case of two-electron systems because of the celebrated fermionic “sign problem” (see, e.g., Refs. 30,31).

The purpose of this paper is to present a detailed study of several hydrogen-bonded dimers (ranging from weak to rather strong bonded-systems) using the perturbational formalism with different levels of description (two different pure perturbational approaches and the hybrid method). More precisely, using the original formalism presented by Hess *et al.*¹² a few years ago we investigate the dependence of the different perturbational contributions on the geometry of the dimer (both the intermonomer distance and the relative orientation) for five different hydrogen-bonded dimers (consisting of H₂O, NH₃, and HF). We discuss in detail the validity of the different representations for the interaction energy presented above and investigate the peculiar role of the second-order exchange-induction energy.

The organization of the present paper is as follows. In section II we give a rapid summary of the formalism used in this work. In particular we give the rather unfamiliar expressions for the exchange-induction and -dispersion energies derived within SAPT theories by Hess *et al.*¹² Section III contains the computational details. In section IV, we present our numerical results for the different contributions of the intermolecular interaction energy and a comparison between the interaction energies obtained with the different approaches. Finally, some conclusions are presented in section V.

II. METHOD

In this section we give a rapid overview of the formalism used in this work; for a very detailed and self-contained presentation the reader is referred to the original work of Hess *et al.*¹² In the perturbation theory of interactions the total Hamiltonian is decomposed as $H = H_0 + V^{AB}$ where H_0 denotes the sum of the non-interacting Hamiltonians of the two monomers *A* and *B* (we shall consider here only dimers, formulas can be trivially generalized to an arbitrary number of monomers) and V^{AB} is the intermolecular interaction potential.

Following standard Symmetry Adapted Perturbation Theories (SAPT) (see, e.g., Refs. 1–3) and using standard notations, the complete first- and second-order interaction energies are written in the form:

$$E^{(1)} = \frac{\langle \Psi_0^A \Psi_0^B | V^{AB} \mathbf{A} | \Psi_0^A \Psi_0^B \rangle}{\langle \Psi_0^A \Psi_0^B | \mathbf{A} | \Psi_0^A \Psi_0^B \rangle}, \quad (4)$$

$$E^{(2)} = - \frac{\langle \Psi_0^A \Psi_0^B | V^{AB} R_0 \mathbf{A} (V^{AB} - E^{(1)}) | \Psi_0^A \Psi_0^B \rangle}{\langle \Psi_0^A \Psi_0^B | \mathbf{A} | \Psi_0^A \Psi_0^B \rangle}, \quad (5)$$

where R_0 denotes the reduced resolvent of H_0 given by

$$R_0 = \sum'_{ij} \frac{|\Psi_i^A \Psi_j^B\rangle \langle \Psi_i^A \Psi_j^B|}{(E_i^A + E_j^B) - (E_0^A + E_0^B)} \quad (6)$$

(the prime in \sum' means as usual that the term corresponding to $i=0$ and $j=0$ is excluded from the summation) and \mathbf{A} is the intersystem antisymmetrizer:

A. Exchange–induction energy

By using Eqs. (11) and (12), $E_{exch-ind}^{(2)}(A \rightarrow B)$ is written as

$$E_{exch-ind}^{(2)}(A \rightarrow B) = -\langle \Psi_0^A \Psi_0^B | (V^{AB} - \langle V^{AB} \rangle) \times (P_{(1)} - \langle P_{(1)} \rangle) | \Psi_0^A \Phi_{ind}^B \rangle, \quad (17)$$

with a similar formula for $E_{exch-ind}^{(2)}(B \rightarrow A)$. A first point is that it is possible to rewrite Φ_{ind}^B in the form:

$$\Phi_{ind}^B = \sum_{k \in B} \Psi_0^B \begin{pmatrix} f_k^B \\ b_k \end{pmatrix}, \quad (18)$$

where the summation runs over all occupied spin orbitals b_k of monomer B and where the so-called “induction functions” f_k^B 's are some well-defined linear combinations of the virtual spin orbitals of B (one associated with each occupied orbital). Using Eq. (18) it is not difficult to show that the exchange induction energy may be now written

$$E_{exch-ind}^{(2)}(A \rightarrow B) = -\sum_{k \in B} ([V^{AB} P_{(1)}]_k - \langle V^{AB} \rangle [P_{(1)}]_k - \langle P_{(1)} \rangle [V^{AB}]_k), \quad (19)$$

with the notation

$$[O]_k \equiv \left\langle \Psi_0^A \Psi_0^B \left| O \right| \Psi_0^A \Psi_0^B \begin{pmatrix} f_k^B \\ b_k \end{pmatrix} \right\rangle, \quad (20)$$

where O stands for an arbitrary operator. Now, by using the fact that the action of the permutation operator $P_{(1)}$ on a product of two determinants Ψ_A and Ψ_B may be expressed as a linear combination of simple products of determinants corresponding to subsystems A and B and by using the Longuet-Higgins representation of the interaction operator V^{AB} (Eqs. (15),(16)) it is possible to show that the three basic contributions in (19) may be written as some specific combinations of electrostatic interactions between some generalized intermolecular charge densities. For example, we obtain for the major contribution¹²

$$[V^{AB} P_{(1)}]_k = \sum_{i \in A} \sum_{\substack{j \in B \\ j \neq k}} \int \int \frac{f_{00}^A \begin{pmatrix} b_j \\ a_i \end{pmatrix} f_{00}^B \begin{pmatrix} f_k^B a_i \\ b_k b_j \end{pmatrix}}{|\mathbf{r}^A - \mathbf{r}^B|} d\mathbf{r}^A d\mathbf{r}^B + \sum_{i \in A} \int \int \frac{f_{00}^A \begin{pmatrix} f_k^B \\ a_i \end{pmatrix} f_{00}^B \begin{pmatrix} a_i \\ b_k \end{pmatrix}}{|\mathbf{r}^A - \mathbf{r}^B|} d\mathbf{r}^A d\mathbf{r}^B, \quad (21)$$

where

$$f_{00}^A \begin{pmatrix} b_j \\ a_i \end{pmatrix} \equiv \left\langle \Psi_0^A \left| \rho^A(\mathbf{r}^A) \right| \Psi_0^A \begin{pmatrix} b_j \\ a_i \end{pmatrix} \right\rangle,$$

with similar definitions for the other generalized charge distributions involved in Eq. (21). Finally, explicit expressions for the generalized charge distributions in terms of mono- and bi-electronic integrals involving spin orbitals a_i, b_j , and f_k^B may be easily obtained.

B. Exchange-dispersion energy

A similar route to that followed for the exchange-induction energy can be used for the exchange-dispersion component. Writing Φ_{disp}^{AB} (see, Eq. (12)) as:

$$\Phi_{disp}^{AB} = \sum_{k \in A} \sum_{l \in B} \sum_{r \in A} \sum_{s \in B} c_{kl}^{rs} \Psi_0^A \begin{pmatrix} a_r \\ a_k \end{pmatrix} \Psi_0^B \begin{pmatrix} b_s \\ b_l \end{pmatrix}, \quad (22)$$

where indices k and l are associated with summations over the corresponding set of *occupied* spin orbitals while s and l refer to summations over the corresponding set of *virtual* spin orbitals and where c_{kl}^{rs} are some coefficients analogous to the linear coefficients of the “induction functions” introduced above, we can express $E_{exch-disp}^{(2)}$ in a form very similar to Eq. (19):

$$E_{exch-disp}^{(2)} = -\sum_{k \in A} \sum_{l \in B} \sum_{r \in A} \sum_{s \in B} c_{kl}^{rs} ([V^{AB} P_{(1)}]_{kl}^{rs} - \langle V^{AB} \rangle [P_{(1)}]_{kl}^{rs} - \langle P_{(1)} \rangle [V^{AB}]_{kl}^{rs}), \quad (23)$$

with the notation

$$[O]_{kl}^{rs} \equiv \left\langle \Psi_0^A \Psi_0^B \left| O \right| \Psi_0^A \begin{pmatrix} a_r \\ a_k \end{pmatrix} \Psi_0^B \begin{pmatrix} b_s \\ b_l \end{pmatrix} \right\rangle. \quad (24)$$

Exactly in the same way as before it is possible to write the elementary contributions of $E_{exch-disp}^{(2)}$ as a combination of some electrostatic interactions between generalized charge distributions which are ultimately written in terms of mono- and bi-electronic integrals. As an example, the major contribution to $E_{exch-disp}^{(2)}$ writes:

$$[V^{AB} P_{(1)}]_{kl}^{rs} = \sum_{\substack{i \in A \\ i \neq k}} \sum_{\substack{j \in B \\ j \neq l}} \int \int \frac{f_{00}^A \begin{pmatrix} a_r b_j \\ a_k a_i \end{pmatrix} f_{00}^B \begin{pmatrix} b_s a_j \\ b_l b_j \end{pmatrix}}{|\mathbf{r}^A - \mathbf{r}^B|} d\mathbf{r}^A d\mathbf{r}^B + \sum_{\substack{i \in A \\ i \neq k}} \int \int \frac{f_{00}^A \begin{pmatrix} a_r b_s \\ a_k a_i \end{pmatrix} f_{00}^B \begin{pmatrix} a_i \\ b_l \end{pmatrix}}{|\mathbf{r}^A - \mathbf{r}^B|} d\mathbf{r}^A d\mathbf{r}^B + \sum_{\substack{j \in B \\ j \neq l}} \int \int \frac{f_{00}^A \begin{pmatrix} b_j \\ a_k \end{pmatrix} f_{00}^B \begin{pmatrix} b_s a_r \\ b_l b_j \end{pmatrix}}{|\mathbf{r}^A - \mathbf{r}^B|} d\mathbf{r}^A d\mathbf{r}^B + \int \int \frac{f_{00}^A \begin{pmatrix} b_s \\ a_k \end{pmatrix} f_{00}^B \begin{pmatrix} a_r \\ b_l \end{pmatrix}}{|\mathbf{r}^A - \mathbf{r}^B|} d\mathbf{r}^A d\mathbf{r}^B, \quad (25)$$

and similar formulas for the other contributions.

III. COMPUTATIONAL DETAILS

A. Dimers

We have studied five different hydrogen-bonded dimers made of the molecules H_2O , NH_3 , and HF . The intramolecular geometry of the monomers has been taken to be the experimental geometry for isolated monomers (water molecule: $R_{OH} = 1.8088$ bohr, $\theta_{HOH} = 104.87^\circ$; ammonia molecule: $R_{NH} = 1.9219$ bohr, $\theta_{HNH} = 107.81^\circ$; HF molecule:

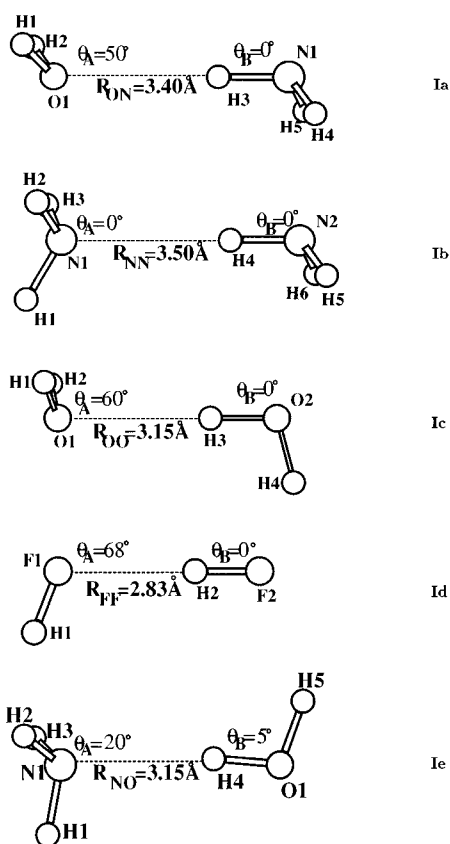


FIG. 1. The five hydrogen-bonded dimers studied. For a definition of the angles θ_A and θ_B , see text.

$R_{\text{HF}} = 1.71362$ bohr). In Figure 1, we present the different dimers in their equilibrium geometry as obtained by the pure perturbational treatment (SAPT, see Eq. (2)), note that slightly different geometries can be obtained with other theoretical schemes, see discussion in the next section. In this work, we shall denote A the proton acceptor molecule and B the proton donor molecule. The dimer geometries will be described by the quantities θ_A , θ_B , and R_{AB} where:

- θ_A defines the angle between the principal axes of the proton acceptor molecule (bisector in H_2O , C_v axis in NH_3 , and bond axis in HF) and the axis $A \cdots B$ connecting the two heavy atoms A and B .
- θ_B is the angle between the B-H bond axis of the proton donor and the axis $A \cdots B$.
- R_{AB} is the (intermolecular) distance between the two heavy atoms A and B of the two monomers. The values of these different quantities at the SAPT equilibrium geometry are given in Figure 1.

The five different dimers have been chosen from very weak to rather strong hydrogen-bonded dimers. The less bounded system is the dimer $\text{H}_2\text{O} \cdots \text{HNH}_2$. In fact, there is no experimental evidence of its existence. It is well-known that NH_3 acts as a proton acceptor when it is involved in a H-bonded system.^{32,33} For example, this is the case for $\text{H}_3\text{N} \cdots \text{HF}$,³⁴ $\text{NCH} \cdots \text{NH}_3$,³⁵ and $\text{HCCH} \cdots \text{NH}_3$.³⁶ There is so far no known example of systems in the gas phase where the

ammonia molecule acts as a proton donor. Here, the $\text{H}_2\text{O} \cdots \text{HNH}_2$ dimer has been studied as a prototype of a H-bonded dimer with NH_3 as a proton donor. A stronger but still weak example of H-bonded dimer is $(\text{NH}_3)_2$. Since the ammonia molecule exhibits no tendency to proton donation, the $(\text{NH}_3)_2$ complex is expected to be a case of H-bonded dimer not easy to treat. In this work a linear H-bonded structure has been chosen for the dimer. Earlier *ab initio* calculations have predicted such a structure.^{37,38} However, this picture is not supported by microwave experiments,^{39,40} which predict a cyclic structure. More recent theoretical (*ab initio*) calculations⁴¹ indicate that cyclic and linear complexes are almost degenerate in energy and that which one is found to be the most stable is extremely sensitive to details of the basis set as well as to the amount of correlation effects included. In fact, three kinds of tunneling motions exist for the ammonia dimer: interchange of the *donor* and *acceptor* roles of the monomers, internal rotation of the monomers about their C_3 symmetry group and *umbrella* inversion tunneling.⁴² A computational exploration of the six-dimensional vibration-rotation-tunneling dynamics of $(\text{NH}_3)_2$ by van Bladel *et al.*⁴³ has concluded that the $(\text{NH}_3)_2$ structure can be obtained from the *ab initio* equilibrium structure by vibrational averaging. Here, the radial evolution of the intermolecular interaction (and its components) of $(\text{NH}_3)_2$ has been mainly studied in order to compare the ammonia dimer with the dimer $\text{HOH} \cdots \text{NH}_3$. The dimers $(\text{H}_2\text{O})_2$ and $(\text{HF})_2$ can be considered as good examples of intermediate H-bonded dimers. Finally, we treat the $\text{H}_3\text{N} \cdots \text{HOH}$ dimer as an example of a rather strong H-bonded system.

B. Basis set

Our calculations for the different dimers have been performed with a very large basis set $(13s \ 8p \ 3d)/(7s \ 2p)$ contracted into $(8s \ 5p \ 3d)/(4s \ 2p)$ (the first set of basis functions corresponds to the heavy atom N, O, or F, the second to the hydrogen atoms). The basis set used has been taken from Voisin⁴⁴ and has been built as follows. First, based on atomic calculations the sets of primitives optimized by van Duijnveltdt $(12s \ 7p)/(6s)$,⁴⁵ have been contracted into some reduced set $(7s \ 4p)/(3s)$. Then, a set of diffuse functions s and p has been added. Their exponents have been obtained according to the averaging procedure presented in Ref. 46. Finally, to better describe the heavy atoms (N, O, and F), three polarization functions d have been added according to the rules proposed by Werner and Meyer.⁴⁷ The two orbitals p of hydrogen are those given by Christiansen and McCullough.⁴⁸ In order to evaluate the quality of our basis set we have performed a number of checks.

1. Basis-set quality: Some monomer properties

The SCF energy and dipole moment have been compared to the some recently estimated Hartree-Fock limits for the three molecules (Table I). Our values for the SCF energies appear to be quite close to the nearly-infinite-basis-set results. The values of the dipole moments are also quite good. It is important to emphasize that reproducing correctly

TABLE I. SCF energies and dipole moments obtained with the basis set used in this work. Comparison with the corresponding near Hartree–Fock limits. All energies in a.u. Dipole moments in Debye.

Molecule	E_{SCF}	$E_{\text{near HF limit}}$	μ_{SCF}	$\mu_{\text{near HF limit}}$
H ₂ O	-76.0606	-76.0673 ^a	1.98	1.98 ^{a,b}
NH ₃	-56.2179	-56.2246 ^a	1.56	1.62 ^a
HF	-100.064	-100.0706 ^a	1.93	1.92 ^a

^aReference 49.

^bReference 53.

the permanent dipole moments is crucial since the interaction energy of hydrogen-bonded systems is dominated by the electrostatic interaction.

2. Basis-set quality: Some dimer properties

a. Complementary exchange energy. A very useful quantity to evaluate the quality of a given finite basis set for computing intermolecular interactions is the so-called “complementary exchange energy.” A very detailed presentation of this quantity can be found in references.^{1,50} However, since the use of this quantity is not very common, let us first give a short presentation of it. The complementary exchange energy, $\epsilon_{\text{compl-exch}}$, is defined via the following formula

$$E_0 \equiv \frac{\langle \Psi_0^A \Psi_0^B | H \mathbf{A} | \Psi_0^A \Psi_0^B \rangle}{\langle \Psi_0^A \Psi_0^B | \mathbf{A} | \Psi_0^A \Psi_0^B \rangle} = \bar{E}_0^0 + \epsilon_{\text{compl-exch}} + \frac{\langle \Psi_0^A \Psi_0^B | V^{AB} \mathbf{A} | \Psi_0^A \Psi_0^B \rangle}{\langle \Psi_0^A \Psi_0^B | \mathbf{A} | \Psi_0^A \Psi_0^B \rangle} \quad (26)$$

where

$$\epsilon_{\text{compl-exch}} = \frac{\langle \Psi_0^A \Psi_0^B | (\bar{E}_0^0 - H_0) \mathbf{A}' | \Psi_0^A \Psi_0^B \rangle}{\langle \Psi_0^A \Psi_0^B | \mathbf{A} | \Psi_0^A \Psi_0^B \rangle}. \quad (27)$$

In Eq. (26) E_0 denotes the total Heitler–London energy and \bar{E}_0^0 the total energy corresponding to the approximate wave function $|\Psi_0^A \Psi_0^B\rangle$ for the unperturbed Hamiltonian H_0 . When Ψ_0^M ($M=A, B$) are chosen to be the exact (ground-state) wave functions of the monomers the complementary exchange energy vanishes and the Heitler–London interaction energy (defined as $E_0 - \bar{E}_0^0$) coincides with the complete first-order interaction energy. Note that, due to the presence of the operator \mathbf{A}' at the numerator, $\epsilon_{\text{compl-exch}}$ decreases exponentially as a function of the distance. This is the reason

why this quantity, which may be viewed as a correction to the ordinary exchange energy, is called “complementary exchange energy.” Now, the important property we shall use is that *within the one-exchange approximation* the complementary exchange energy vanishes if and only if the approximate functions used for the unperturbed monomers are the exact Hartree–Fock solutions. Since for not too small intermonomer distances the exact and one-exchange complementary exchange energies are almost identical $\epsilon_{\text{compl-exch}}$ is a good indicator of how far an approximate SCF wave function built from some given basis set is from the Hartree–Fock limit. Of course, for very small values of $\epsilon_{\text{compl-exch}}$ it would be necessary to consider the true one-exchange complementary energy instead of $\epsilon_{\text{compl-exch}}$. In Table II we present for the different dimers treated the values obtained for $\epsilon_{\text{compl-exch}}$ at a few representative distances R_{AB} . To compare with, we also report the values of the Heitler–London exchange energy defined as

$$E_{\text{exch-HL}}^{(1)} = E_{\text{exch}}^{(1)} + \epsilon_{\text{compl-exch}}. \quad (28)$$

The values obtained for $\epsilon_{\text{compl-exch}}$ are found to be rather small when compared with typical values (see, e.g., Refs. 1 or 51). This illustrates the good quality of the basis sets used in this work.

b. Counterpoise correction at the SCF level. In a supermolecular calculation of a complex the better the basis set used for describing each monomer is, the smaller the basis-set-superposition error (BSSE) is. We have computed this error by using the standard counterpoise method of Boys and Bernardi,⁵² some of our results are displayed in Table III. As a general rule, we get a very small counterpoise correction.

c. Second-order dispersion energy. Szalewicz *et al.*⁵³ pointed out that the use of f functions improved considerably the dispersion energy. Their estimate of the exact value was -2.0 kcal/mol for the water dimer near the equilibrium distance ($R_{O\dots O} = 3. \text{ \AA}$). In a recent work, Rybak *et al.*²⁰ have obtained a value of -1.90 kcal/mol by using a very large basis set. Here, although no f functions are present in our calculations, our 122 atomic-orbital dimer basis set leads, for the water dimer, to a value of -1.89 kcal/mol which is almost identical to the value obtained by Rybak *et al.* and quite close to the exact one estimated by Szalewicz *et al.*

TABLE II. Complementary exchange energy $\epsilon_{\text{compl-exch}}$ and first-order Heitler–London exchange energy $E_{\text{exch-HL}}^{(1)}$ for some representative values of the distance R_{AB} between the heavy atoms. Energies in kcal/mol, distances in Å.

R_{AB}		H ₂ O...HNH ₂	H ₃ N...HNH ₂	H ₂ O...HOH	HF...HF	H ₃ N...HOH
2.75	$\epsilon_{\text{compl-exch}}$	-0.05	0.43	-0.22	-0.30	0.03
	$E_{\text{exch-HL}}^{(1)}$	19.70	30.49	12.80	4.91	19.84
3.00	$\epsilon_{\text{compl-exch}}$	-0.16	-0.10	-0.15	-0.26	-0.10
	$E_{\text{exch-HL}}^{(1)}$	8.12	13.69	5.18	1.78	8.72
3.70	$\epsilon_{\text{compl-exch}}$	0.00	0.01	0.02	-0.02	0.00
	$E_{\text{exch-HL}}^{(1)}$	0.64	1.40	0.40	0.09	0.85

TABLE III. Counterpoise-corrected SCF interaction energy, ΔE_{CP}^{SCF} , and counterpoise correction, ϵ_{CP} for some representative distances. Energies in kcal/mol. Distances in Å.

R_{AB}		H ₂ O...HNH ₂	H ₃ N...HNH ₂	H ₂ O...HOH	HF...HF	H ₃ N...HOH
2.75	ΔE_{CP}^{SCF}	3.84	5.84	-2.46	-3.64	-2.78
	ϵ_{CP}	0.09	0.10	0.10	0.20	0.10
3.00	ΔE_{CP}^{SCF}	-0.01	0.60	-3.65	-3.48	-4.54
	ϵ_{CP}	0.05	0.06	0.06	0.16	0.06
3.70	ΔE_{CP}^{SCF}	-1.38	-1.73	-2.50	-1.90	-3.29
	ϵ_{CP}	0.02	0.03	0.02	0.11	0.02

IV. PERTURBATIONAL RESULTS

A. Total interaction energies at equilibrium geometries

In Table IV we present the total interaction energies obtained for the different dimers studied. We also present the optimized geometries, R_{AB} , θ_A , and θ_B . We have used three different approaches:

- (i) The pure perturbational approach, SAPT, including all perturbational components up to the second-order

$$\Delta E_{int}^{SAPT} = E_{RS}^{(1)} + E_{exch}^{(1)} + E_{ind}^{(2)} + E_{exch-ind}^{(2)} + E_{disp}^{(2)} + E_{exch-disp}^{(2)}. \quad (29)$$

- (ii) A truncated approach we shall refer to in the following as SAPT_{trunc} in which the exchange part of the induction is neglected (this method will play an important role in the discussion to follow)

$$\Delta E_{int}^{SAPT_{trunc}} = E_{RS}^{(1)} + E_{exch}^{(1)} + E_{ind}^{(2)} + E_{disp}^{(2)} + E_{exch-disp}^{(2)}. \quad (30)$$

- (iii) The hybrid approach mixing the SCF interaction en-

ergy (counterpoise-corrected) and the complete dispersion contribution calculated with SAPT:

$$\Delta E_{int}^{hybrid} = \Delta E_{int}^{SCF} + E_{disp}^{(2)} + E_{exch-disp}^{(2)}. \quad (31)$$

For the three different approaches the geometries have been optimized by varying the angles θ_I ($I=A$ and B) and the distance R_{AB} around the estimated equilibrium geometry (θ_I within -30° and $+30^\circ$ around θ_I^{exp} using $\pm 5^\circ$ steps, R_{AB} within -0.40 Å and 0.4 Å around R_{AB}^{exp} with 0.03 Å steps).

From a qualitative point of view, both SAPT, SAPT_{trunc}, and the hybrid methods lead essentially to the same results. The force of the hydrogen bond (importance of the total interaction energy) for the dimers we have studied may be classified as follows: H₂O...HNH₂ < H₃N...HNH₂ < H₂O...HOH ~ HF...HF < H₃N...HOH, where the notation $X < Y$ means that the dimer X is less bounded than the dimer Y . We verify the well-known result that NH₃ acts preferentially as a proton acceptor rather than a proton donor since here H₃N...HOH is much more stable than H₂O...HNH₂. Note also that NH₃ acts as a better acceptor than H₂O since

TABLE IV. Intermolecular interaction energy, ΔE_{int} , obtained from different methods (see text) at the corresponding equilibrium geometry. The values of θ_A , θ_B , and R_{AB} are given together with the known experimental values. Energies in kcal/mol, distances in bohr.

	H ₂ O...HNH ₂	H ₃ N...HNH ₂	H ₂ O...HOH	HF...HF	H ₃ N...HOH
ΔE_{int}^{SAPT}	-2.09	-2.50	-4.22	-3.75	-5.19
$\Delta E_{int}^{SAPT_{trunc}}$	-2.50	-3.15	-5.45	-5.82	-7.55
ΔE_{int}^{hybrid}	-2.49	-3.13	-5.31	-4.89	-6.76
ΔE_{int}^{exp}	^a	^b	-5.4 ± 0.7^c	-4.9 ± 0.1^d	$\sim 6^e$
R_{eq}^{SAPT}	3.40	3.50	3.15	2.83	3.15
$R_{eq}^{SAPT_{trunc}}$	3.20	3.20	2.68	2.48	2.70
R_{eq}^{hybrid}	3.25	3.30	2.91	2.68	2.93
R_{eq}^{exp}	^a	^b	2.98 ^f	2.68 ^g	2.99 ^h
θ_A	50°	0°	60°	68°	20°
θ_A^{exp}	^a	^b	60° ^f	62° ^g	11° < θ_A < 23° ^h
θ_B	0°	0°	0°	0°	5°
θ_B^{exp}	^a	^b	0° ^f	11° ^g	$\approx 13^{\circ h}$

^aUnphysical molecule, see text.

^bLinear H-bonded structure, no experimental values, see text.

^cReference 55.

^dReference 20.

^eTo our knowledge no experimental value available. The value quoted is an *ab initio* estimate given by Latajka and Scheiner (Ref. 56).

^fReference 57.

^gReference 58.

^hReference 59.

$\text{H}_3\text{N}\dots\text{HOH}$ is more stable than $\text{H}_2\text{O}\dots\text{HOH}$. Concerning the geometrical parameters it appears that the value of the angle θ_A defining the angle between the axes $A\dots B$ (A and B being the heavy atoms of the complex) and the principal axis of the proton acceptor depends strongly on the chemical nature of the acceptor. A value of about 60° has been obtained when the proton acceptor is H_2O or HF . A smaller value is obtained when the proton acceptor is NH_3 . The value of the angle θ_B characterizing the position of the bond $A\text{-H}$ (A being N , O , or F) of the proton acceptor is always very close to 0° . The smallest distance $R_{A\dots B}$ between the two heavy atoms at the equilibrium geometry has been obtained for the HF dimer. We get the following series: $R_{\text{F}\dots\text{F}}(\text{HF})_2 < R_{\text{O}\dots\text{O}}(\text{H}_2\text{O})_2 < R_{\text{N}\dots\text{N}}(\text{NH}_3)_2$. The equilibrium distance $R_{A\dots B}$ calculated for the heterodimer involving NH_3 and H_2O increases from the most stable dimer ($\text{H}_3\text{N}\dots\text{HOH}$) to the less stable one ($\text{H}_2\text{O}\dots\text{HNNH}_2$).

From a more quantitative point of view, the first important point to note is that values of the interaction energy, ΔE_{inter} , depend appreciably on the method used and/or the dimer considered. First, it is clear that $\Delta E_{\text{int}}^{\text{SAPT}}$ is always smaller in magnitude than $\Delta E_{\text{int}}^{\text{hybrid}}$ or $\Delta E_{\text{int}}^{\text{SAPT}_{\text{trunc}}}$. The systematic difference is about 20%. The comparison between $\Delta E_{\text{int}}^{\text{SAPT}_{\text{trunc}}}$ and $\Delta E_{\text{int}}^{\text{hybrid}}$ depends on the dimer. We can distinguish three different cases:

(i) the weak H-bonded dimers case (including $\text{H}_2\text{O}\dots\text{HNNH}_2$ and $(\text{NH}_3)_2$) for which $\Delta E_{\text{int}}^{\text{SAPT}_{\text{trunc}}}$ and $\Delta E_{\text{int}}^{\text{hybrid}}$ almost coincide.

(ii) the intermediate case of medium H-bonded dimers ($(\text{H}_2\text{O})_2$ and $(\text{HF})_2$) for which we obtain two different results. For the $(\text{H}_2\text{O})_2$ dimer the total interaction energy calculated with $\text{SAPT}_{\text{trunc}}$ and the hybrid methods are almost identical (the difference is less than 3%). This is a result which has already been obtained by Refs. 4, 12, and 20. However, this is no longer true for the $(\text{HF})_2$ dimer for which $\Delta E_{\text{int}}^{\text{SAPT}_{\text{trunc}}}$ and $\Delta E_{\text{int}}^{\text{hybrid}}$ are off by about 20%, therefore, the equality of these two quantities cannot be considered as a general rule. We shall return to this important point later after having presented the individual components of the interaction energy (sec. C below).

(iii) the rather strong H-bonded dimer, $\text{H}_3\text{N}\dots\text{HOH}$, for which an important difference between the truncated and hybrids results is observed.

Regarding the equilibrium distance R_{eq} we find that the SAPT results are systematically larger than those obtained with the two other methods. Once again, the situation is not so clear when we compare the values obtained with $\text{SAPT}_{\text{trunc}}$ and the hybrid methods. Almost identical results have been obtained for the case of weakly bonded dimers while shorter distances have been calculated with the $\text{SAPT}_{\text{trunc}}$ approach for the other dimers. If we compare with the known experimental values it is clear that the hybrid method is the method which gives the most plausible results. Now, regarding the calculated angular parameters (θ_A and θ_B) defining the relative position of the two molecules within the H-bonded dimer we have systematically obtained almost the same values with the three different procedures. We have also found that not only the equilibrium angles are

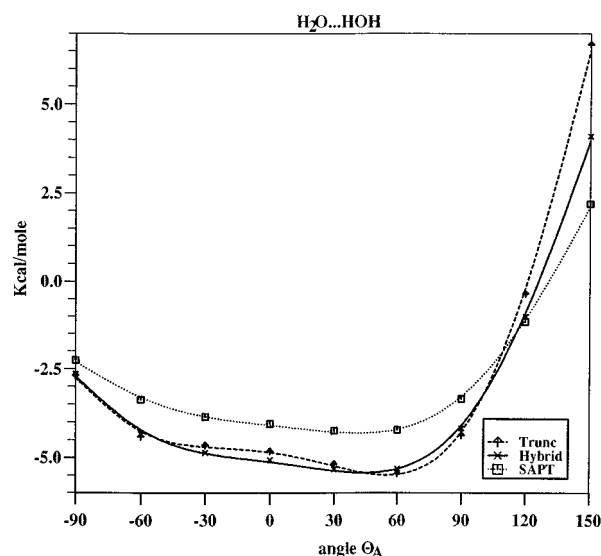


FIG. 2. Interaction energy curves, ΔE_{int} , as a function of θ_A (see text) for the water dimer as calculated by SAPT, $\text{SAPT}_{\text{trunc}}$, and the hybrid methods.

very similar but also the general shape of the interaction energy curves with respect to the relative angles for all dimers presented here. To illustrate this point we present in Figure 2 the energy curve obtained for the water dimer as a function of the angle θ_A . Clearly, there exists some important radial dependence of the interaction energy on the procedure used but a much smaller one for the relative position of the molecules. In what follows we study in more detail this radial dependence.

B. Radial dependence of the perturbational contributions

Keeping the angular parameters θ_A and θ_B of each dimer fixed at their optimized values, we have investigated the radial dependence of the intermolecular interaction energy perturbational components.

Our main purpose is to study which contributions to the interaction energy are actually dominant in stabilizing the five studied complexes. We are also interested to trace back to its origin the poor stability of the dimer $(\text{NH}_3)_2$ and also the very short $\text{F}\dots\text{F}$ distance in the $(\text{HF})_2$ dimer.

In the next few tables we present the radial dependence of the following contributions:

- (i) $E_{\text{RS}}^{(1)}$, $E_{\text{exch}}^{(1)}$ and the complete first-order, $E^{(1)\text{SAPT}}$ (Table V);
- (ii) the second-order induction energy $E_{\text{ind}}^{(2)}$, its exchange part $E_{\text{exch-ind}}^{(2)}$, and the complete induction energy $E_{\text{ind}}^{(2)\text{SAPT}}$ (Table VI);
- (iii) the second-order dispersion energy $E_{\text{disp}}^{(2)}$, its exchange part $E_{\text{exch-disp}}^{(2)}$, and the complete dispersion energy $E_{\text{disp}}^{(2)\text{SAPT}}$ (Table VII).

We make the following comments on the results presented in Tables V–VII:

- (i) All contributions of the Rayleigh–Schrödinger (RS) treatment (no exchange terms), namely $E_{\text{RS}}^{(1)}$, $E_{\text{ind}}^{(2)}$, and

TABLE V. First-order Rayleigh–Schrödinger energy, $E_{RS}^{(1)}$, first-order exchange energy, $E_{exch}^{(1)}$, and complete first-order, $E_{SAPT}^{(1)} = E_{RS}^{(1)} + E_{exch}^{(1)}$ for different values of R_{AB} . Energies in kcal/mol and distances in Å.

R_{AB}		H ₂ O...HNH ₂	H ₃ N...HNH ₂	H ₂ O...HOH	HF...HF	H ₃ N...HOH
2.75	$E_{RS}^{(1)}$	-11.28	-17.00	-11.51	-6.63	-16.36
	$E_{exch}^{(1)}$	19.75	30.07	13.10	5.21	19.87
	$E_{SAPT}^{(1)}$	8.48	13.08	1.59	-1.42	3.44
2.90	$E_{RS}^{(1)}$	-7.62	-12.00	-8.40	-5.16	-12.30
	$E_{exch}^{(1)}$	11.40	18.90	7.40	2.98	12.23
	$E_{SAPT}^{(1)}$	3.78	6.90	-1.00	-2.18	-0.07
3.00	$E_{RS}^{(1)}$	-6.20	-9.60	-7.15	-4.42	-10.27
	$E_{exch}^{(1)}$	8.32	13.80	5.33	2.04	8.83
	$E_{SAPT}^{(1)}$	2.12	4.20	-1.82	-2.38	-1.44
3.17	$E_{RS}^{(1)}$	-4.32	-6.71	-5.39	-3.47	-7.72
	$E_{exch}^{(1)}$	4.54	8.02	2.84	1.06	5.03
	$E_{SAPT}^{(1)}$	0.22	1.31	-2.55	-2.41	-2.70
4.00	$E_{RS}^{(1)}$	-1.24	-1.76	-1.94	-1.39	-2.61
	$E_{exch}^{(1)}$	0.21	0.52	0.12	0.03	0.31
	$E_{SAPT}^{(1)}$	-1.03	-1.24	-1.82	-1.36	-2.30

$E_{disp}^{(2)}$, have a stabilizing effect. Of course, the major contribution is the electrostatic interaction energy which represents between 55 and 70 % of the total RS contribution. When we compare the relative force of the RS interaction energy for the different H-bonded dimers we get the following order: $(\text{NH}_3)_2 \approx \text{H}_3\text{N}\dots\text{HOH} < \text{H}_2\text{O}\dots\text{HNH}_2 \approx (\text{H}_2\text{O})_2 < (\text{HF})_2$. For an average distance of $R_{AB} = 3$ Å, it appears that for the dimers $(\text{H}_2\text{O})_2$ and $(\text{HF})_2$ the electrostatic energy represents 75% and 50% of the value obtained for $(\text{NH}_3)_2$; for the dimers $(\text{H}_2\text{O})_2$ and $(\text{HF})_2$, $E_{ind}^{(2)}$ represents 75% and 40% of the value obtained for $(\text{NH}_3)_2$, respectively; and for $(\text{H}_2\text{O})_2$ and $(\text{HF})_2$ $E_{disp}^{(2)}$ represents, 50% and 20% of $E_{disp}^{(2)}$ of $(\text{NH}_3)_2$, respectively.

(ii) The total first- and total second-order exchange contributions (including both induction and dispersion contributions) reduce the stabilizing effect of the Rayleigh–Schrödinger terms just discussed. As expected, the major exchange contribution results from the first-order exchange term which represents 80% of the total exchange contribu-

tion at intermediate distances, while the second-order induction and dispersion exchange components have been obtained to represent 14% and 6% of the total exchange, respectively. Regarding the total exchange contribution we obtain the following order: $(\text{NH}_3)_2 > (\text{H}_2\text{O}\dots\text{HNH}_2) \approx (\text{H}_3\text{N}\dots\text{HOH}) > (\text{H}_2\text{O})_2 > (\text{HF})_2$. We have investigated the behavior of each individual exchange component as a function of the distance R_{AB} . We have found that for distances greater than 3 Å the exchange contribution may be very well represented via a single exponential function, $Ce^{-\alpha(R-R_0)}$. The set of parameters obtained for the different dimers and for the different components of the exchange part using the results for $R_{AB} = 3.00, 3.17, 3.70,$ and 4.00 Å are given in Table VIII (note that R_0 has been chosen to be fixed at 3 Å). The values of the parameters depend essentially on the nature of the exchange contribution (first-order, exchange-induction or exchange-dispersion) and on the chemical nature of the molecules involved in the complex.

TABLE VI. Second-order induction energy, $E_{ind}^{(2)}$, second-order exchange induction energy, $E_{ind-exch}^{(2)}$, and complete second-order induction, $E_{ind}^{(2)SAPT} = E_{ind}^{(2)} + E_{ind-exch}^{(2)}$ for different values of R_{AB} . Energies in kcal/mol and distances in Å.

R_{AB}		H ₂ O...HNH ₂	H ₃ N...HNH ₂	H ₂ O...HOH	HF...HF	H ₃ N...HOH
2.75	$E_{ind}^{(2)}$	-6.10	-9.59	-4.55	-2.39	-7.58
	$E_{ind-exch}^{(2)}$	4.27	6.30	2.81	1.36	4.70
	$E_{ind}^{(2)SAPT}$	-1.83	-3.29	-1.74	-1.03	-2.88
2.90	$E_{ind}^{(2)}$	-3.26	-5.69	-2.49	-1.38	-4.63
	$E_{ind-exch}^{(2)}$	2.17	3.61	1.40	0.70	2.74
	$E_{ind}^{(2)SAPT}$	-1.09	-2.08	-1.00	-0.68	-1.89
3.00	$E_{ind}^{(2)}$	-2.30	-4.04	-1.80	-0.96	-3.36
	$E_{ind-exch}^{(2)}$	1.48	2.49	0.95	0.45	1.91
	$E_{ind}^{(2)SAPT}$	-0.82	-1.55	-0.85	-0.51	-1.45
3.17	$E_{ind}^{(2)}$	-1.22	-2.30	-1.00	-0.54	-1.99
	$E_{ind-exch}^{(2)}$	0.71	1.32	0.45	0.20	1.04
	$E_{ind}^{(2)SAPT}$	-0.51	-0.98	-0.55	-0.34	-0.95
4.00	$E_{ind}^{(2)}$	-0.10	-0.21	-0.10	-0.06	-0.21
	$E_{ind-exch}^{(2)}$	0.02	0.07	0.02	0.01	0.06
	$E_{ind}^{(2)SAPT}$	-0.08	-0.14	-0.08	-0.05	-0.15

TABLE VII. Second-order dispersion energy, $E_{disp}^{(2)}$, second-order exchange dispersion energy, $E_{disp-exch}^{(2)}$, and complete second-order dispersion energy, $E_{disp}^{(2)SAPT} = E_{disp}^{(2)} + E_{disp-exch}^{(2)}$ for different values of R_{AB} . Energies in kcal/mol and distances in Å.

R_{AB}		H ₂ O...HNNH ₂	H ₃ N...HNNH ₂	H ₂ O...HOH	HF...HF	H ₃ ...HOH
2.75	$E_{disp}^{(2)}$	-4.63	-6.78	-3.38	-1.46	-4.82
	$E_{disp-exch}^{(2)}$	1.28	2.28	0.82	0.24	1.35
	$E_{disp}^{(2)SAPT}$	-3.35	-4.50	-2.56	-1.22	-3.47
2.90	$E_{disp}^{(2)}$	-3.19	-4.88	-2.32	-1.00	-3.45
	$E_{disp-exch}^{(2)}$	0.77	1.45	0.48	0.14	0.88
	$E_{disp}^{(2)SAPT}$	-2.42	-3.43	-1.84	-0.86	-2.57
3.00	$E_{disp}^{(2)}$	-2.59	-3.93	-1.89	-0.79	-2.77
	$E_{disp-exch}^{(2)}$	0.57	1.07	0.34	0.09	0.64
	$E_{disp}^{(2)SAPT}$	-2.02	-2.86	-1.55	-0.70	-2.13
3.17	$E_{disp}^{(2)}$	-1.79	-2.74	-1.31	-0.53	-1.93
	$E_{disp-exch}^{(2)}$	0.33	0.64	0.19	0.05	0.38
	$E_{disp}^{(2)SAPT}$	-1.46	-2.10	-1.13	-0.48	-0.92
4.00	$E_{disp}^{(2)}$	-0.34	-0.54	-0.24	-0.10	-0.38
	$E_{disp-exch}^{(2)}$	0.02	0.05	0.01	0.00	0.03
	$E_{disp}^{(2)SAPT}$	-0.32	-0.49	-0.23	-0.10	-0.35

(iii) Clearly, at very short distances the repulsive exchange part of the first-order dominates the attractive RS contribution. However, at sufficiently large distances the exchange part vanishes and only the electrostatic term survives (it behaves as $1/R_{AB}^3$). Accordingly, the total first-order energy displays a minimum. The location of the minimum depends very much on the system studied. Looking at results of Table V we see that the weak H-bonded dimer (NH₃)₂ has a shallow minimum at a relatively large distance (-1.30 kcal/mol with $R_{eq} \approx 3.8$ Å). In contrast, the stronger-bonded dimers (H₂O)₂ and (HF)₂ have a larger total first-order interaction energy (about -2.50 kcal/mol). The minimum region of (HF)₂ is found to be quite broad within a range of values between 2.9 Å and 3.3 Å.

(iv) The positive (repulsive) exchange contributions, $E_{exch-ind}^{(2)}$ and $E_{exch-disp}^{(2)}$ terms never dominate their Rayleigh-Schrödinger counterparts, $E_{ind}^{(2)}$ and $E_{disp}^{(2)}$. In fact, the second-order RS terms tend to decrease the intermolecular interaction energy and to push the equilibrium distance R_{AB} towards shorter distances, this effect is slightly reduced by the second-order exchange terms whose main effect is to bring back R_{AB} to more reasonable values. The effect of the

second-order exchange contributions is more important for (NH₃)₂ than for the (HF)₂ dimer (see Tables IV, VI, and VII). In conclusion, the relative stability between the different H-bonded dimers results from a subtle balance between Rayleigh-Schrödinger and total exchange contributions.

C. Radial dependence of the total interaction energy: A comparison between the different approaches

In Table IX we present the total interaction energy as calculated within SAPT, SAPT_{trunc} and the hybrid methods (Eqs. (29), (30), and (31)) as a function of R_{AB} . We also present in Figures 3 and 4 the complete interaction energy curves for two representative examples: the NH₃ and HF dimers. A number of remarks are in order. First, it is clear that at very large distances the three approaches give the same results for the total interaction energy and thus, the same dissociative behavior. The results obtained by the different methods at small and intermediate distances may be quite different depending on the force of the hydrogen bond. For the two weak H-bonded cases (H₂O...HNNH₂ and (NH₃)₂) the agreement between the truncated and hybrid

TABLE VIII. Parameters of the representation $Ce^{-\alpha(R-R_0)}$ ($R_0=3$ Å) for: (a) the first-order exchange energy, (b) the second-order exchange induction energy, (c) the second-order exchange dispersion energy. Parameters C in kcal/mol and α in Å⁻¹.

	H ₂ O...HNNH ₂	H ₃ N...HNNH ₂	H ₂ O...HOH	HF...HF	H ₃ N...HOH
$E_{exch}^{(1)}$					
α	3.685	3.280	3.777	4.205	3.351
C	8.404	13.910	5.397	2.121	8.860
$E_{exch-ind}^{(2)}$					
α	4.317	3.585	3.906	5.489	3.450
C	1.473	2.444	0.893	0.474	1.893
$E_{exch-disp}^{(2)}$					
α	3.392	3.053	3.518	3.115	3.085
C	0.572	1.077	0.344	0.088	0.636

TABLE IX. Total interaction energy calculated with SAPT, SAPT_{trunc} and the hybrid methods, see text. Energies in kcal/mol and distances in Å.

R_{AB}		H ₂ O...HNH ₂	H ₃ N...HNH ₂	H ₂ O...HOH	HF...HF	H ₃ N...HOH
2.54	ΔE_{int}^{SAPT}	11.29	15.31	1.60	-2.41	2.79
	$\Delta E_{int}^{SAPT_{trunc}}$	1.31	2.04	-5.11	-5.73	-7.14
	ΔE_{int}^{hybrid}	6.63	9.15	-2.51	-4.45	-2.84
2.75	ΔE_{int}^{SAPT}	3.31	5.26	-2.71	-3.67	-2.90
	$\Delta E_{int}^{SAPT_{trunc}}$	-0.96	-1.00	-5.51	-5.03	-7.60
	ΔE_{int}^{hybrid}	0.50	1.35	-5.02	-4.86	-6.26
2.90	ΔE_{int}^{SAPT}	0.27	1.39	-3.94	-3.72	-4.53
	$\Delta E_{int}^{SAPT_{trunc}}$	-1.90	-2.22	-5.34	-4.42	-7.27
	ΔE_{int}^{hybrid}	-1.48	-1.29	-5.31	-4.51	-6.74
3.00	ΔE_{int}^{SAPT}	-0.72	-0.21	-4.20	-3.59	-5.02
	$\Delta E_{int}^{SAPT_{trunc}}$	-2.19	-2.70	-5.10	-4.03	-6.93
	ΔE_{int}^{hybrid}	-2.03	-2.25	-5.19	-4.18	-6.68
3.17	ΔE_{int}^{SAPT}	-1.76	-1.75	-4.22	-3.23	-5.19
	$\Delta E_{int}^{SAPT_{trunc}}$	-2.46	-2.97	-4.68	-3.42	-5.57
	ΔE_{int}^{hybrid}	-2.47	-2.98	-4.73	-3.57	-6.15
3.70	ΔE_{int}^{SAPT}	-1.83	-2.27	-2.84	-2.01	-3.72
	$\Delta E_{int}^{SAPT_{trunc}}$	-1.90	-2.52	-2.89	-2.02	-3.88
	ΔE_{int}^{hybrid}	-1.92	-2.53	-2.90	-2.07	-3.88
4.00	ΔE_{int}^{SAPT}	-1.43	-1.87	-2.13	-1.51	-2.82
	$\Delta E_{int}^{SAPT_{trunc}}$	-1.45	-1.93	-2.14	-1.51	-2.86
	ΔE_{int}^{hybrid}	-1.46	-1.96	-2.16	-1.53	-2.88

results is very good except at small distances (see Figure 3). For the rather strong dimers (HF)₂ and H₂O...HOH the truncated and hybrid curves appear to differ quite substantially by about 20%. The water dimer appears as an intermediate species for which both methods are in reasonable agreement, a result which has been already obtained by Refs. 4, 12, and 20. It should be noticed that for strong enough dimers the equilibrium distance obtained with the truncated method is systematically smaller than with the hybrid method. Regarding the SAPT results it is clear that ΔE_{int}^{SAPT} is always smaller in magnitude than ΔE_{int}^{hybrid} or $\Delta E_{int}^{SAPT_{trunc}}$. The systematic difference for all dimers is about 20%. Note also that the equilibrium distance obtained by the pure perturbational method is also systematically greater than with the two other methods. In order to discuss further these results it is impor-

tant to point out that the equality of the results obtained with the truncated and hybrid methods should result from the following equality:

$$\Delta E_{int}^{SCF} \sim E^{(1)} + E_{ind}^{(2)}, \quad (32)$$

where $E^{(1)}$ is the complete first-order (electrostatic and exchange terms) and $E_{ind}^{(2)}$ is the Rayleigh–Schrödinger part of the induction energy. It has been argued that this equality should result from a fortunate cancellation between the exchange part of the induction energy and some part of the higher-order perturbational contributions which are implicitly included in a SCF supermolecular calculation of the interaction energy.⁴ Despite the fact that it is roughly true for the water dimer, our results clearly demonstrate that it is wrong for the (HF)₂ and H₃N...HOH dimers. To illustrate

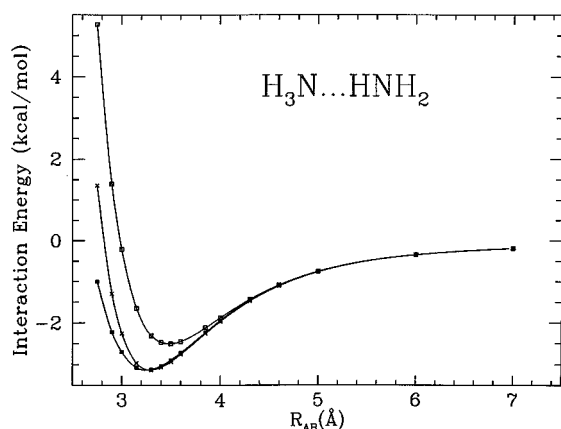


FIG. 3. Interaction energy curves, ΔE_{int} , as a function of R_{AB} for the (NH₃)₂ dimer as calculated by SAPT (curve with open squares), SAPT_{trunc} (solid squares), and the hybrid methods (crosses).

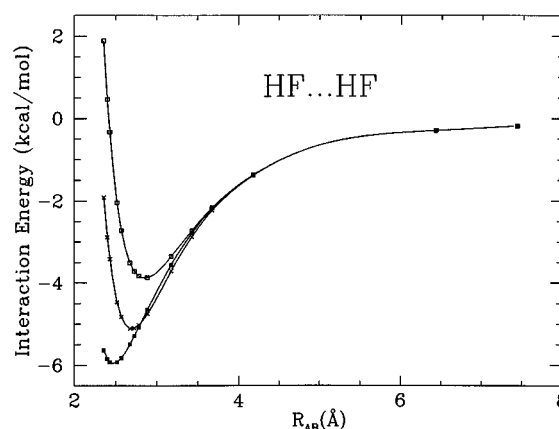


FIG. 4. Interaction energy curves, ΔE_{int} , as a function of R_{AB} for the (HF)₂ dimer as calculated by SAPT (curve with open squares), SAPT_{trunc} (solid squares), and the hybrid methods (crosses).

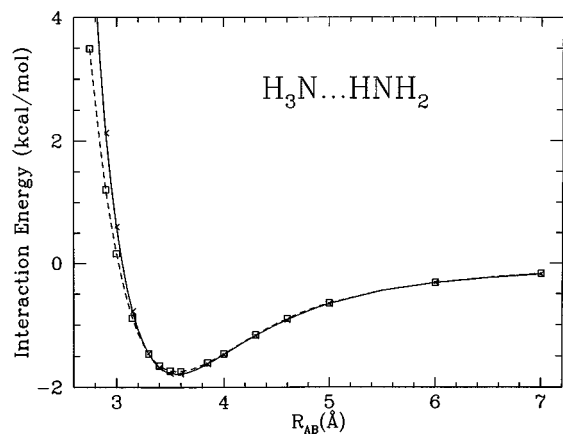


FIG. 5. Comparison between the SCF interaction energy curve (solid line with crosses) and the curve representing the perturbational sum $E^{(1)} + E_{ind}^{(2)}$ (dashed line with open squares) for the $(\text{NH}_3)_2$ dimer.

this point we present in Figures 5 and 6 a comparison between the SCF interaction energy curve and the curve representing the perturbational sum $E^{(1)} + E_{ind}^{(2)}$ for the $(\text{NH}_3)_2$ and $(\text{HF})_2$ dimers, respectively. For the NH_3 dimer the overall agreement between the two curves is strikingly good. In contrast, for the $(\text{HF})_2$ dimer there is a clear disagreement, the main feature being an important difference in the location of the minimum. Although the difference of minimum energies is small (about 0.2 kcal/mol) this difference at the new corresponding minima is magnified when the total dispersion energy is added to lead to the complete interaction energy. Following the Morokuma decomposition (see e.g., Ref. 54) the SCF interaction energy may be written as:

$$\Delta E_{int}^{SCF} = E_{elec} + E_{exch-HL} + E_{ind}^{SCF}, \quad (33)$$

where E_{elec} is the electrostatic energy (identical to $E_{RS}^{(1)}$) as calculated here with SAPT, $E_{exch-HL}$ is the Heitler–London exchange energy which reduces almost to $E_{exch}^{(1)SAPT}$ when a very large basis set is used (see discussion on the complementary exchange in Sec. III.B) and E_{ind}^{SCF} is by definition the

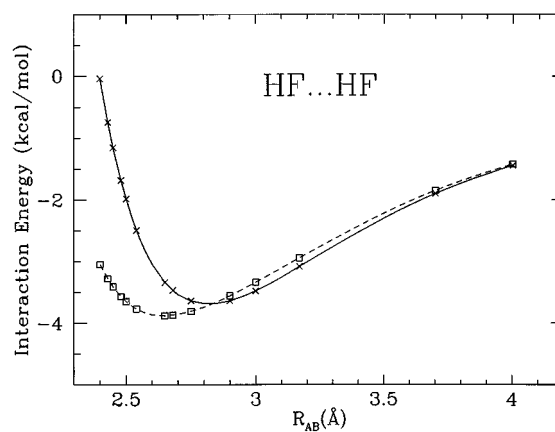


FIG. 6. Comparison between the SCF interaction energy (solid line with crosses) and the curve representing the perturbational sum $E^{(1)} + E_{ind}^{(2)}$ (dashed line with open squares) for the $(\text{HF})_2$ dimer.

induction part of the SCF interaction energy. In order to discuss the status of the SAPT induction energy (including or not the exchange contribution) with respect to the SCF induction energy, we have presented in Table X the SCF induction energy, the difference between the SCF induction energy and the total SAPT induction energy (including exchange effects) and the same difference without the exchange terms, all quantities being given as a function of the distance R_{AB} . It immediately appears that at short and intermediate distances, the three calculated values of the induction energy are different. The nice agreement obtained for the water dimer at $R_{O...O} = 3 \text{ \AA}$ between E_{ind}^{SCF} and $E_{ind}^{(2)}$ is actually fortuitous. In fact, E_{ind}^{SCF} should not be compared to $E_{ind}^{(2)}$ because the so-called *apparent correlation* or self-consistency effects are included in the supermolecular Hartree–Fock interaction energy but not in our computation of $E_{ind}^{(2)}$.¹⁵ As emphasized by Sadlej¹⁵ the second-order RS induction energy calculated within SAPT methodology by using the first-order perturbed wave function is equivalent to that computed within a UnCoupled Hartree–Fock (UCHF)

TABLE X. Comparison between the SCF induction energy and the perturbational induction energy. Energies in kcal/mol and distances in Å.

R_{AB}		$\text{H}_2\text{O}\dots\text{H}_2\text{O}$	$\text{H}_3\text{N}\dots\text{H}_2\text{N}$	$\text{H}_2\text{O}\dots\text{HOH}$	$\text{HF}\dots\text{HF}$	$\text{H}_3\text{N}\dots\text{HOH}$
2.75	E_{ind}^{SCF}	-4.57	-7.66	-3.84	-1.92	-6.26
	$E_{ind-tot}^{(2)} - E_{ind}^{SCF}$	2.74	4.37	2.10	0.89	3.39
	$E_{ind}^{(2)} - E_{ind}^{SCF}$	-1.53	-1.93	-0.71	-0.47	-1.32
2.90	E_{ind}^{SCF}	-2.61	-4.75	-2.25	-1.15	-4.00
	$E_{ind-tot}^{(2)} - E_{ind}^{SCF}$	1.52	2.67	1.25	0.47	2.11
	$E_{ind}^{(2)} - E_{ind}^{SCF}$	-0.65	-0.94	-0.24	-0.23	-0.63
3.00	E_{ind}^{SCF}	-1.93	-3.49	-1.68	-0.84	-3.00
	$E_{ind-tot}^{(2)} - E_{ind}^{SCF}$	1.11	1.94	0.83	0.33	1.55
	$E_{ind}^{(2)} - E_{ind}^{SCF}$	-0.37	0.55	-0.12	-0.12	-0.36
3.17	E_{ind}^{SCF}	-1.10	-2.00	-0.99	-0.50	-1.85
	$E_{ind-tot}^{(2)} - E_{ind}^{SCF}$	0.59	1.02	0.44	0.16	0.90
	$E_{ind}^{(2)} - E_{ind}^{SCF}$	-0.12	-0.30	-0.01	-0.04	-0.14
3.70	E_{ind}^{SCF}	-0.23	-0.48	-0.23	-0.13	-0.46
	$E_{ind-tot}^{(2)} - E_{ind}^{SCF}$	0.08	0.20	0.07	0.03	0.18
	$E_{ind}^{(2)} - E_{ind}^{SCF}$	0.01	0.01	0.02	0.02	0.01

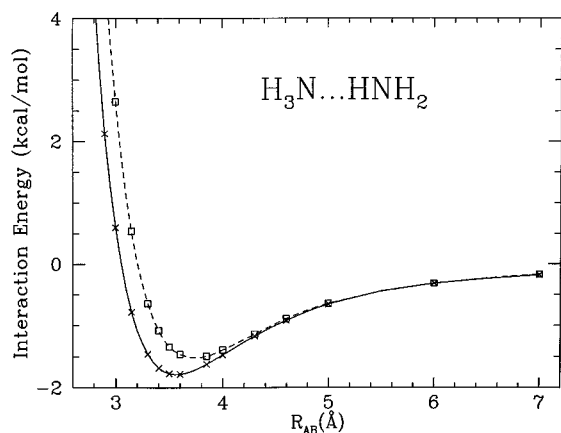


FIG. 7. Comparison between the SCF interaction energy curve (solid line with crosses) and the curve representing the perturbational sum $E^{(1)} + E_{ind}^{(2)} + E_{exch-ind}^{(2)}$ (dashed line with open squares) for the $(\text{NH}_3)_2$ dimer.

perturbation scheme. In particular, the perturbation-induced modification of the Hartree–Fock (HF) potential is not taken into account. In a UCHF scheme, the results obtained for $E_{ind}^{(2)}$ are underestimated. Sadlej emphasizes that if both unperturbed and perturbed many-electron systems are described in the HF approximation, then the appropriate perturbation theory is the Coupled Hartree–Fock (CHF) scheme. The induction computed at the CHF level is usually denoted as $E_{ind,resp}^{(2)}$, it sums up to infinity certain linear diagrams without rings and then fully accounts for the self-consistency effects. The CHF scheme corrects the HF potential of the unperturbed systems but no correlation corrections are introduced. The total exchange-induction contributions are also present in the SCF induction energy. However, at the SCF level, once again because of the self-consistency effects we get $E_{exch-ind,resp}^{(2)}$ instead of $E_{exch-ind}^{(2)}$. Finally, the SCF induction contribution is written as:

$$\Delta E_{ind}^{SCF} = E_{ind,resp}^{(2)} + E_{exch-ind,resp}^{(2)} + \delta E_{mixt}, \quad (34)$$

where δE_{mixt} gathers all higher perturbational terms. A number of calculations of $E_{ind,resp}^{(2)}$ and $E_{exch-ind,resp}^{(2)}$ have been presented (see references in Ref. 28).

Although results obtained with the hybrid approach are good it is important to realize that escaping from a pure perturbational treatment has some drawbacks. How much of the higher-order perturbational contributions, what part of the exchange-induction energy, etc... is recovered from a SCF supermolecular calculation is not easy to estimate. It may be argued that the good results obtained with the hybrid approach could result from a subtle balance between neglected contributions very different in nature. It is not clear whether that balance will still hold when higher-order contributions will be evaluated. Of course, a similar problem is present in a pure perturbational scheme but it is important to emphasize that the neglected quantities not taken into account are much more clearly identified. Accordingly, in our opinion it is still important to study the pure perturbational treatments. From Tables IV and IX (in particular the comparisons with experimental values) it appears that the complete pure perturbational treatment (SAPT) is the approach

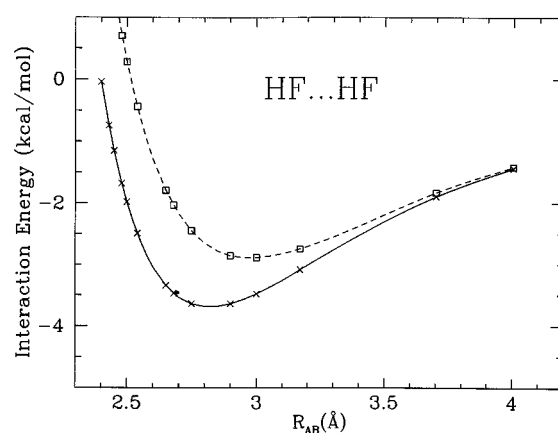


FIG. 8. Comparison between the SCF interaction energy curve (solid line with crosses) and the curve representing the perturbational sum $E^{(1)} + E_{ind}^{(2)} + E_{exch-ind}^{(2)}$ (dashed line with open squares) for the $(\text{HF})_2$ dimer.

which gives the less plausible results. Results from the truncated approach demonstrate that the main part of the disagreement between ΔE_{int}^{SAPT} on one hand, and $\Delta E_{int}^{SAPT, trunc}$ and ΔE_{int}^{hybrid} on the other hand, comes from the second-order exchange-induction energy which destroys the overall quality of the results. To illustrate this point Figures 7 and 8 display a comparison between the ΔE_{int}^{SCF} curve and the curve representing the perturbational sum $E^{(1)} + E_{ind}^{(2)} + E_{exch-ind}^{(2)}$ for the dimers $\text{H}_3\text{N}\dots\text{HNH}_2$ and $(\text{HF})_2$ (same curves as in Figures 5 and 6, except that the exchange-induction energy has been added). In Figure 7 it is seen that the very good agreement found in Figure 5 is destroyed. This result shows that the calculated values for $E_{exch-ind}^{(2)}$ are overestimated since for a weak dimer such as $\text{H}_3\text{N}\dots\text{HNH}_2$ the perturbational contributions beyond the second-order should be small and a perturbational description should be adequate. For stronger dimers like $(\text{HF})_2$ the clear disagreement between the two curves does not necessarily mean that we are in trouble (higher-order terms certainly play a role) but there is no reason not to believe that, in that case also, the exchange-induction term has been overestimated. Let us have a closer look to our estimate of the exchange-induction energy. Within the one-exchange approximation used in this work $E_{exch-ind}^{(2)}$ is calculated as a sum of three terms (see Sec. II, Eq. (19)). The analysis of our results has shown that the first term is positive and represents the major part of $E_{exch-ind}^{(2)}$ while the sum of the second and third terms is negative and essentially reduces $E_{exch-ind}^{(2)}$ by a quantity which depends on R_{AB} . For instance, for the $\text{H}_3\text{N}\dots\text{HOH}$ dimer this quantity has been calculated to be 24%, 15% and 11% for $R_{AB} = 2.54 \text{ \AA}$, 2.75 \AA , and 2.93 \AA , respectively. Quite similar results have been obtained with the other dimers. The sum of the two last terms entering into $E_{exch-ind}^{(2)}$ (see Eq. (19)) may be rewritten as

$$E_{RS}^{(1)} \sum_k \left[\sum_{i \in A} S_{ij}^{AB} S_{ik}^{AB} + \sum_{j \in B} S_{jk}^{AB} S_{jk}^{AB} \right] + E_{ind}^{(2)} \sum_{i \in A} \sum_{j \in B} |S_{ij}^{AB}|^2. \quad (35)$$

From Eq. (35) we see that an underestimation of the last term related to the induction part leads to an overestimation of the

exchange-induction energy. If, as emphasized by Sadlej,¹⁵ the induction part is underestimated within the SAPT treatment, then, it is plausible that there exists some reducing effect for the exchange-induction energy related to the induction part. In other words, higher-order terms (related to the apparent correlation effects) would contribute significantly to the total exchange-induction energy. Besides this effect, we can also argue that the one-exchange approximation is only valid for intermediate and large intermolecular distances and some bias could be introduced by neglecting multiple exchanges. The neat effect of the neglect of multiple exchange terms is not easy to estimate.

Finally, we would like to end with some remarks about the intramonomer correlation effects on the results presented here. Quite recently a number of studies have addressed the problem of evaluating the intramonomer correlations contributions to the interaction energy.^{11,13,20,22–28} Although a complete knowledge of all contributions is not at our disposal, the calculations made so far show clearly the importance of such effects. Of course, this is expected for the electrostatic energy of hydrogen-bonded systems which depends essentially on the magnitude of the permanent dipoles of the molecules known to be overestimated at the SCF level. However, it is more surprising to get even stronger corrections for the exchange contribution to the first-order.¹³ Some important effects (about 0.5 kcal/mol) have also been obtained for the dispersion and induction part (-0.42 kcal/mol for $E_{disp}^{(22)}$ and -0.60 kcal/mol for $E_{ind}^{(22)}$ in the case of the water dimer,²⁰ the second superscript indicating the perturbational order in the Møller-Plesset expansion). These results are of particular importance for the discussion just presented on the exchange-induction. As mentioned above, an underestimation of the induction energy leads to an overestimation of the exchange-induction. Accordingly, the neat effect of the intramonomer correlation could be a reduction of the exchange-induction energy. However, it should be noted that there is an opposite trend for the electrostatic energy, although this effect is probably less pronounced. This discussion illustrates the fact that there is still much room left to fully understand the intricate balance between the different contributions to the interaction energy.

V. CONCLUSIONS

In this work we have presented a detailed perturbational study of several hydrogen-bonded dimers consisting of H₂O, NH₃, and HF molecules. Three different approaches have been used to compute the interaction energy: a pure perturbational approach, ΔE_{int}^{SAPT} , including all perturbational components up to the second-order calculated at the SCF level, a so-called truncated approach, $\Delta E_{int}^{SAPT_{trunc}}$, in which the exchange part of the induction is not considered, and the hybrid approach, ΔE_{int}^{hybrid} , in which the supermolecular SCF interaction energy (counterpoise-corrected) is supplemented by the complete dispersion contribution calculated with SAPT (both Rayleigh-Schrödinger and exchange contributions). The quality of the large basis sets used has been checked by computing a number of properties for both the monomers and the corresponding dimers (SCF monomer

energies, dipole moments, complementary exchange energies, etc...). From a qualitative point of view, the physical results obtained with the three approaches are essentially similar. The relative force of the different hydrogen bonds are in agreement with experimental results and, in particular, the acceptor or donor properties are correctly reproduced. From a quantitative point of view, a number of differences emerge when using the different approaches. These quantitative differences are particularly important for the radial properties, much less for the angular ones. A general result already emphasized by some authors is that, at the level of approximation employed here (SCF level, perturbational components up to the second-order only, etc.), the hybrid approach seems to be the most reliable approach (see Table IV). The pure perturbational approach including the main contributions up to the second-order (calculated at the SCF level) gives the less plausible results. Clearly, some of the neglected contributions must be introduced to get better results. In particular, the second-order exchange-induction energy is certainly overestimated. We have argued that this quantity is very probably reduced by some intramonomer correlation contribution. However, it is important to emphasize that the error on the known experimental quantities is in general of the same order of magnitude as the dispersion of the results obtained using the different approaches. Accordingly, there is still no clearcut conclusion on which method is the best at the present time. To analyze further the importance of each perturbational components is therefore essential if we want to reach in a controlled way the asymptotic regime of the perturbational expansion of the intermolecular interaction energy.

ACKNOWLEDGMENT

The authors are grateful to the “Institut du Développement et des Ressources en Informatique Scientifique” (IDRIS) for providing them with computer time.

¹P. Arrighini, in *Intermolecular Forces and their Evaluation by Perturbation Theory*, Lectures Notes in Chemistry (Springer-Verlag, Berlin, 1981).

²B. Jeziorski and W. Kolos, in *Molecular Interactions*, edited by H. Ratajczak and W. J. Orville-Thomas (Wiley, New York, 1982), Vol. 3.

³I. G. Kaplan, in *Theory of Molecular Interactions* (Elsevier, Amsterdam, 1986), Vol. 42.

⁴B. Jeziorski and M. van Hemert, *Mol. Phys.* **31**, 713 (1976).

⁵G. Chalasiniski, *Mol. Phys.* **49**, 1353 (1983).

⁶G. Chalasiniski and B. Jeziorski, *Mol. Phys.* **32**, 81 (1976).

⁷G. Chalasiniski and B. Jeziorski, *Theor. Chim. Acta* **46**, 277 (1977).

⁸G. Chalasiniski, *Chem. Phys.* **82**, 207 (1983).

⁹G. Chalasiniski, *Chem. Phys. Lett.* **86**, 165 (1982).

¹⁰S. Rybak, Ph.D. thesis, University of Warsaw, Warsaw, 1988.

¹¹B. Jeziorski, R. Moszynski, S. Rybak, and K. Szalewicz, in *Proceedings of the Symposium on Many-Body Methods, Tel-Aviv, Israel, 1988*, edited by U. Kaldor (Springer-Verlag, Berlin, 1989).

¹²O. Hess, M. Caffarel, C. Huiszoon, and P. Claverie, *J. Chem. Phys.* **92**, 6049 (1990).

¹³R. Moszynski, B. Jeziorski, and K. Szalewicz, *J. Chem. Phys.* **100**, 1312 (1994).

¹⁴G. Chalasiniski and B. Jeziorski, *Int. J. Quantum Chem.* **7**, 63 (1973).

¹⁵A. J. Sadlej, *Mol. Phys.* **39**, 1249 (1980).

¹⁶R. Moszynski, S. M. Cybulski, and G. Chalasiniski, *J. Chem. Phys.* **100**, 4998 (1994).

¹⁷S. M. Cybulski, *J. Chem. Phys.* **96**, 8225 (1992).

¹⁸S. M. Cybulski, *J. Chem. Phys.* **97**, 7545 (1992).

¹⁹M. Jaszunski, *Mol. Phys.* **39**, 777 (1980).

